

Research Article

A comparative study of fouling-free nanodiamond and nanocarbon electrochemical sensors for sensitive bisphenol A detection

Luyun Jiang ^{a,1}, Ibon Santiago ^{b,*}, John Foord ^{a,**}^a Department of Chemistry, University of Oxford, Chemistry Research Laboratory, Mansfield Rd, Oxford, OX1 3TA, UK^b Physics Department, Technical University of Munich, Am Coulombwall 4a, 85748 Garching b, München, Germany

ARTICLE INFO

Article history:

Received 30 September 2020

Received in revised form

21 November 2020

Accepted 24 November 2020

Available online 2 December 2020

Keywords:

Boron-doped diamond

Nanocarbon

Electrochemical sensors

Bisphenol

ABSTRACT

Bisphenol A (BPA) is a chemical found in polycarbonate plastics and epoxy resins which is biologically harmful and toxicologically relevant at low doses. Electrochemical sensors offer rapid and accurate detection of bisphenols but suffer from electrode fouling. Boron-doped diamond is known for its exceptional capability to resist chemical fouling due to the weak molecular adsorption of sp^3 carbon. In this work, we use nanodiamond to overcome electrode fouling and detect BPA with a low detection limit at 5 nM. Further, we demonstrate the use of nanocarbon-modified electrodes for BPA detection. One-time use nanocarbon electrodes detect BPA through direct oxidation of BPA in a sensitive and reproducible fashion. For continuous monitoring of BPA, we introduce a new approach based on the detection of the by-product of BPA oxidation, hydroquinone (HQ), which acts as a proxy for BPA quantitation without the need of electrode replacement. These findings aim to tackle the challenges of increasing concern of BPA food and water contamination, as an alternative to the more costly and time consuming central laboratory tests.

© 2020 Elsevier Ltd. All rights reserved.

1. Introduction

Bisphenol A (BPA), also known as 2,2-(4,4-dihydroxydiphenyl) propane, is a cheap and durable synthetic compound used widely in industry. The widespread use of BPA in polycarbonate consumer products like cans and bottles has led to an increased BPA exposure in food, drinks and water [1]. A similar structure to endocrine hormones like estradiol and diethylstilbestrol makes BPA an endocrine-disrupting compound (EDC) [2]. Exposure to excess amounts of BPA in humans is known to cause diabetes, cardiovascular diseases, breast and prostate cancer, reduced fertility and liver damage [3,4]. BPA also poses a threat to aquatic environments preventing the normal growth and development of many aquatic species [5]. Concerns about the health impact of BPA have led regulatory bodies around the world to restrict its use. Many countries have banned BPA in polycarbonate infant feeding bottles [6]. The Food and Drug Administration (FDA) set a dose limitation of BPA at 40 $\mu\text{g}/\text{kg}$ body weight (bw)/day [7] and it is regulated to 4 $\mu\text{g}/$

kg bw/day by the European Food Safety Authority [8]. However, a recent finding from the Consortium Linking Academic and Regulatory Insights on BPA Toxicity (CLARITY BPA) revealed a significant increase of mammary cancer incidence in rodents at doses of BPA administered (2.5 $\mu\text{g}/\text{kg}$ bw/day) [9]. The study suggests that even low doses of BPA are biologically harmful and toxicologically relevant. Efficient measurement of low levels of BPA is therefore paramount to reduce BPA exposure.

BPA detection is usually carried out in central labs with expensive and time-consuming methods such as liquid chromatography (HPLC, UPLC) [10,11], gas chromatography (GC) or mass spectrometry (MS) [12–14]. The detection limits of these methods can be down to the order of nanomolar but require special sample preparation and treatment. Colourimetric enzyme-linked immunosorbent assays (ELISA) [15] are used commercially to detect BPA. These assays require multiple steps, long operation times and have a short lifetime due to the use of enzymes. Their sensitivity and reproducibility are low compared with GC/MS tests carried out in central

* Corresponding author.

** Corresponding author.

E-mail addresses: ibon.santiago@tum.de (I. Santiago), john.foord@chem.ox.ac.uk (J. Foord).¹ These authors contributed equally.

labs. The demand for BPA detection at community settings away from centralised labs is increasing, therefore a low-cost, sensitive and accurate sensor that allows on-site monitoring would be beneficial.

Electrochemical BPA sensors have attracted great interest in the past decade as a promising technology for on-site monitoring of BPA. They benefit from speed, simple operation and low-cost equipment. Electrochemical BPA sensors include metal nanoparticles [16–18], carbon-based particles [1,19,20], organic framework-based [13,21], aptasensors [22] and enzymes [23]. The most common principle of operation relies on the oxidation of BPA into 1,4-Benzoquinone and formaldehyde. Most BPA electrochemical sensors oxidise BPA at a potential of +0.4–0.6 V [1,24], with a detection limit on the order of micromolar, which reduces their effectiveness significantly. BPA forms an electropolymerized film on electrode surfaces, resulting in larger double-layer capacitance and lower electrode sensitivity. Electrode surface fouling is affected by several factors such as the concentration of the analyte, pH of the solution and the choice of surfactant agents. Electrode fouling is the main bottleneck preventing more sensitive detection and continuous operation [13,25,26].

Nanodiamond consists of crystallised sp^3 diamond carbon doped with boron, making it a conductive material, known as boron-doped diamond (BDD). The versatility of BDD has enabled its use as electrodes for a wide range of electrochemical and analytical applications [27]. BDD electrodes offer advantageous properties such as high stability and oxidation power, wide potential windows, reduced background current and rapid charge transfer [28]. In particular, BDD electrodes are favoured for systems suffering from high interference and electrode fouling due to the low electrochemical reactivity of nanodiamond and weak molecular adsorption.

This work presents three methods to detect BPA electrochemically while avoiding the detrimental effects of electrode fouling. We achieve this first by using boron-doped nanodiamond modified electrodes known for their low fouling properties (Fig. 1 a). Another way to eliminate the effect of fouling is by using single-use electrodes. Nanocarbon electrodes, while susceptible to electrode fouling, offer low-cost, easy fabrication and highly reproducible BPA sensors (Fig. 1 b). To completely circumvent electrode fouling, we devised an indirect detection method for the first time. The nanocarbon electrode oxidises BPA first into quinone, and it then detects the redox reaction of quinone to quantify the initial BPA concentration (Fig. 1 c). This indirect method enables continuous monitoring of BPA at nanocarbon electrodes.

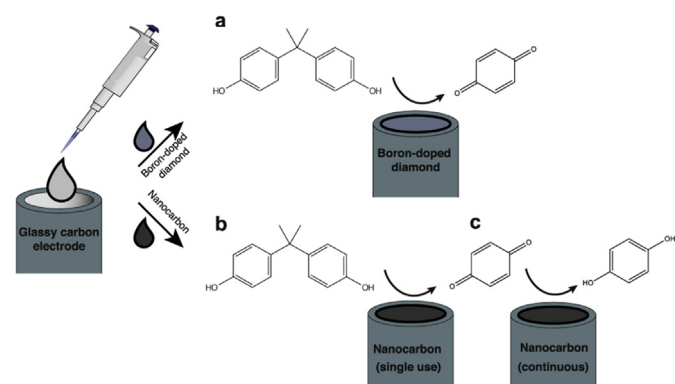


Fig. 1. Scheme of electrode modification and Bisphenol A detection methods in this work. (a) Electrode modified by nanodiamond detects the oxidation of bisphenol A. (b) Electrode modified by nanocarbon detects the oxidation of bisphenol A. Each measurement was carried out at single-use electrodes. (c) Electrode modified by nanocarbon detects the by-product hydroquinone.

2. Experimental methods

2.1. Materials

The commercial Monarch 430 amorphous carbon (Cabot Corporation, CB M 430) was purchased from James M Brown Ltd (Staffordshire, UK). Nanodiamond powder (ND-105/G4) was acquired from Yorkshire Bioscience Ltd. Bisphenol A powder was purchased from Sigma Aldrich. Other chemicals were obtained from Sigma-Aldrich of A.C.A. reagent grade unless otherwise stated.

2.2. Electrode preparation

Glassy carbon electrodes were cleaned before use by polishing with alumina powder, which was then removed by ultrasonication in water for 3 min. A total of 5 g milling beads were mixed with 1 mg powder of amorphous carbon or nanodiamond powder and 5 mL Milli-Q water. The mixture was sonicated for 12 h, and then centrifuged three times for 5 min at 10,000 rpm. 10 μ l carbon materials suspensions were drop-coated onto a glassy carbon electrode with a surface area of 0.0707 cm^2 and subsequently dried under a fume hood. A physical characterisation of the nanodiamond electrode can be found in our previous work [29–31].

2.3. Electrochemical measurements

Electrochemical measurements were performed at room temperature (20 ± 2 °C) with μ -AUTOLAB III potentiostat (Eco-Chemie, Netherlands), running GPES software (Version 4.9). A three-electrode system was used consisting of a working electrode, a Pt wire as counter-electrode and an Ag/AgCl reference electrode. Experiments were carried out in 0.1 M phosphate buffer solution (pH 7.4). All solutions and subsequent dilutions were prepared with Milli-Q water ($> 18 \text{ M}\Omega\text{cm}$). Square wave voltammetry (SWV) was performed at a frequency of 10 Hz, a sensitivity of 1 mV and an amplitude of 10 mV.

3. Results and discussion

3.1. BPA detection at nanodiamond electrode

Electrodes were prepared following the drop-casting method, illustrated in Fig. 1 and described in Experimental methods. We first characterised BPA oxidation through cyclic voltammetry at a glassy carbon electrode (GCE), nanodiamond-GCE (ND-GCE) and nanocarbon-GCE (NC-GCE) (SI Fig. 1). An oxidation peak appears at ca. +0.54 V in 0.2 mM BPA. The peak currents are highest at NC-GCE, followed by ND-GCE, also observed in our previous work

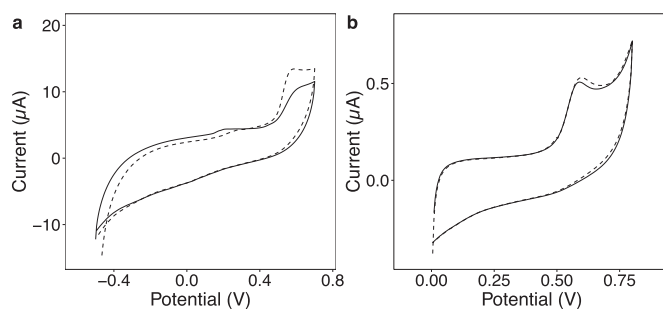


Fig. 2. Cyclic voltammograms of the first (solid line) and the second scans (dashed line) in an electrolyte containing 0.1 M phosphate buffer and 0.2 mM BPA at (a) bare GCE; (b) ND-GCE, with a scan rate of 50 mVs^{-1} . (A colour version of this figure can be viewed online.)

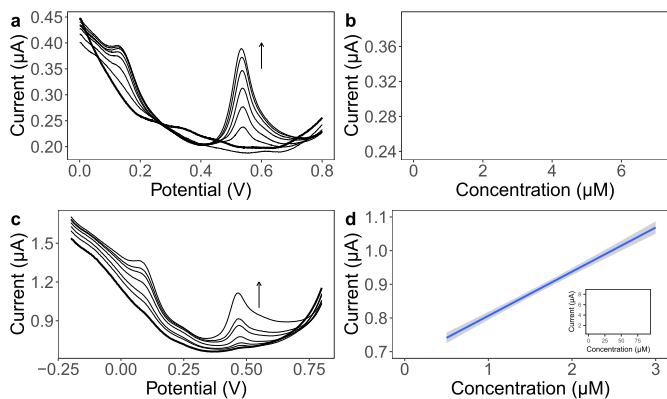


Fig. 3. Square wave voltammograms of increasing BPA in 0.1 M phosphate buffer at (a) bare GCE, (c) ND-GCE, scanning from 0 to 0.8 V; (b) and (d) show the resulting plots of peak current vs. BPA concentration.

with other phenolic compounds [31]. However, the BPA oxidation peak reduces by 80% at the GCE after sequential CV scans (Fig. 2 a). This decrease is due to electrode fouling caused by electropolymerisation of BPA [25,32].

Both ND-GCE and NC-GCE show enhancement in BPA oxidation peak current. For ND-GCE, the main enhancement is from the reduced noise, which dropped from 1 nA to 0.21 nA, while the sensitivity increased from $0.03 \mu\text{A}\mu\text{M}^{-1}$ to $0.13 \mu\text{A}\mu\text{M}^{-1}$. As for NC-GCE, the main contribution to an enhanced peak current is the increase in sensitivity from $0.03 \mu\text{A}\mu\text{M}^{-1}$ to $0.3 \mu\text{A}\mu\text{M}^{-1}$. The main difference is due to the interaction of electrodes with the analytes. NC-GCE shows stronger adsorption than bare GCE while the ND-GCE adsorbs less strongly. The strong adsorption of BPA on NC-GCE leads to a high oxidation current, likely due to the porous structure of nanocarbon. As for ND-GCE, its sp^3 carbon limits the adsorption of electrolytes and slows down the electrokinetics, resulting in low background current, reduced noise and fouling.

In contrast, the BPA oxidation decreases by less than 20% at the ND-GCE (Fig. 2 b), indicative of low electrode fouling. Weak adsorption of polar functional groups on the nonpolar surface of nano-diamond causes minimal surface fouling [31], which enables the use of ND-GCE to detect BPA. To study the electrochemical behaviour of BPA at the ND-GCE surface, we carried out cyclic voltammetry at scan rates from 20 to 200 mVs^{-1} (SI Fig. 2). The linear relationship between peak current and scan rate indicates that the main contribution to the measured current is coming from adsorbed BPA at the surface, rather than by diffusion from the bulk. The surface coverage for all electrodes is reported in SI Fig. 8.

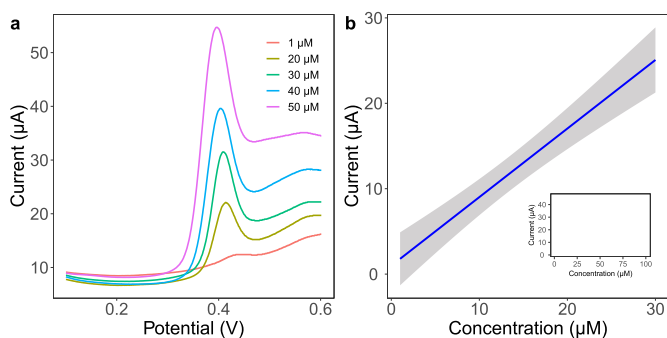


Fig. 4. (a) Square wave voltammograms at freshly prepared NC-GCE in 0.1 M phosphate buffer and 1, 10, 20, 30 and 50 μM BPA respectively and (d) plots of peak current vs. BPA concentration. (A colour version of this figure can be viewed online.)

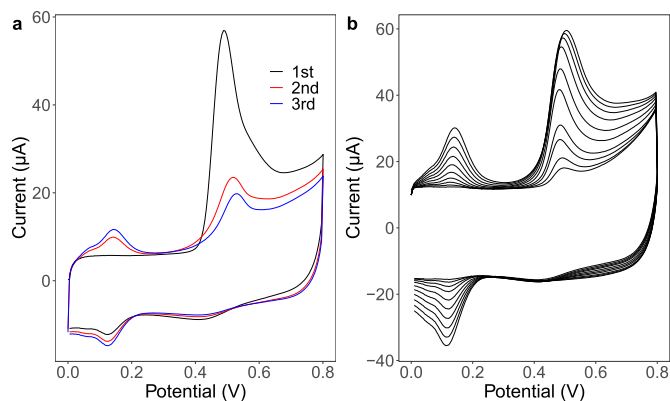


Fig. 5. (a) Cyclic voltammograms of consecutive scans, (i) first, (ii) second and (iii) third, in electrolyte containing 0.2 mM BPA and 0.1 M phosphate buffer at NC-GCE; (b) cyclic voltammograms at NC-GCE in 0.1 M phosphate buffer with the sequential addition of BPA from 0 to 200 μM . (A colour version of this figure can be viewed online.)

We used square wave voltammetry (SWV) in a potential window from +0 to +0.8 V to detect BPA at ND-GCE. Continuous addition of BPA yielded the voltammograms and the resulting plots of peak height vs. concentration of BPA at GCE (Fig. 3 a and b) and ND-GCE (Fig. 3 c and d).

ND-GCE displayed a linear response in a range between 0.1 μM and 50 μM and sensitivity of $0.13 \mu\text{A}\mu\text{M}^{-1}$, calculated as the ratio of current and concentration. The detection limit was 5 nM ($S/N=3$). The low detection limit at ND-GCE is due to low noise, i.e. the fluctuation of non-faradaic current in the absence of BPA.

3.2. BPA detection at single-use nanocarbon electrode

Different from the weak adsorption of nanodiamond, NC-GCE is an efficient electrochemical sensor for phenolic compounds due to the high signal resulting from strong adsorption. This is supported by the linear dependence between peak current and scan rate, as shown in SI Fig. 6. However, direct detection of BPA using NC-GCE is limited due to strong electrode fouling. SI Fig. 3 shows that the detection range only reached 4 μM , making it not suitable for continuous environmental BPA monitoring.

We circumvent this limitation by using single-use electrodes for each experiment. This approach is possible for NC-GCE due to its

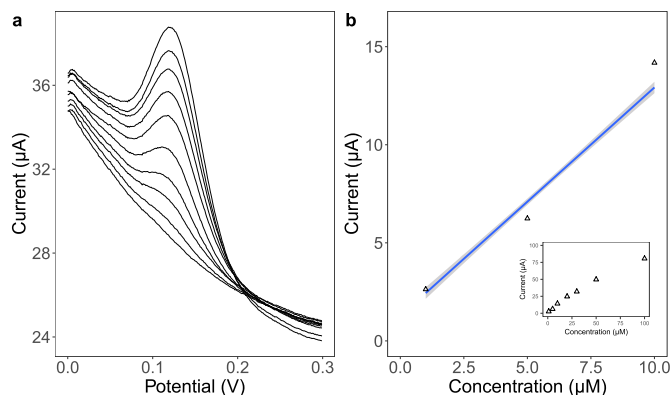


Fig. 6. (a) Square wave voltammograms in solution containing 0.1 M phosphate buffer with sequential addition of BPA from 1 to 10 μM (after initial oxidation at +0.6 V for 60 s) at NC-GCE and the (b) plots of peak current vs. BPA concentration (added concentrations are represented by a triangle). (A colour version of this figure can be viewed online.)

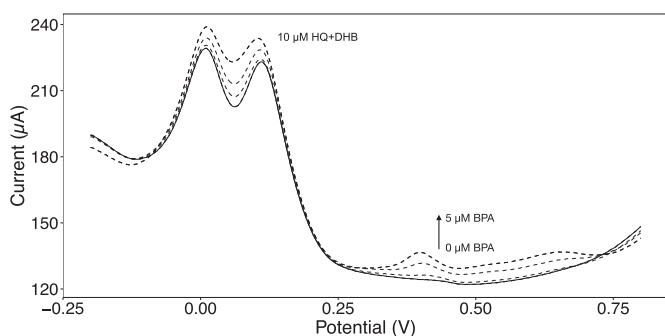


Fig. 7. The square wave voltammograms in solution containing 0.1 M phosphate buffer, 10 μM HQ and DHB and increasing concentration of BPA at NC-GCE.

low-cost and facile electrode modification. Fresh NC-GCE electrodes were prepared before each measurement following the procedure in Experimental methods. Fig. 4 demonstrates that freshly prepared electrodes detect BPA in solution in a concentration range from 0 to 30 μM with a detection limit of 0.56 μM and sensitivity of 0.85 $\mu\text{A}\mu\text{M}^{-1}$. To test the reproducibility, ten NC-GCE separate sensors were prepared and tested with the same BPA solution, yielding a measurement error of less than 5%.

3.3. Indirect BPA detection at nanocarbon electrode via quinone redox reaction

The previous methods detect the oxidation of BPA directly, which is the mechanism adopted by most of the reported electrochemical BPA sensors. Such an approach is vulnerable to fouling because the cyclic sweep up to a high potential (above +1 V) leads to electropolymerisation and prevents further BPA oxidation at the surface. Here we propose another method to use NC-GCE for BPA sensing by detecting the secondary redox reaction corresponding to quinone and hydroquinone (HQ), which is a by-product of BPA oxidation (Fig. 1 c). GC-MC analysis indicates that BPA oxidation results in three intermediate products, among which quinone is the main by-product [33,34]. This is in agreement with the experimental observation that the redox potentials of the BPA oxidation by-product and that of HQ co-localise, as shown in SI Fig. 9. Due to

the strong adsorption of quinone by nanocarbon, the by-product is strongly attracted to the electrode surface, thereby facilitating its detection. This indirect measurement of BPA allows for continuous use of NC-GCE.

Fig. 5 shows the emergence of a secondary peak at +0.1 V, after an initial sweep to oxidise BPA. Continuous scans up to 10 cycles show that a plateau is reached after three scans. At the same time, the secondary peak increases continuously (SI Fig. 4). The result shows that a clean NC-electrode rapidly loses the ability to oxidise BPA efficiently due to fouling but retains the ability to respond to quinones which develop in the solution even when fouling occurs. This opens the door to the possibility of detecting BPA through the secondary peak. First, BPA was oxidised at +0.6 V for 30 s to generate the HQ as a by-product. Then SWV was carried out at a lower potential from +0 to +0.3 V to detect HQ adsorbed on the NC-GCE surface.

Fig. 5 b displays CVs at NC-GCE in 0.1 M phosphate buffer with continuous addition of BPA from 0 to 200 μM , and the resulting plots of peak current vs. BPA concentration are shown in SI Fig. 5. All experiments were performed at the same electrode. The peaks corresponding to BPA oxidation and quinone/hydroquinone redox were observed at +0.6 V and +0.1 V, respectively. Sequential addition of BPA resulted in a linear increase in the peak current of the secondary redox reaction (SI Fig. 5b). On the contrary, the BPA oxidation peak is nonlinear (SI Fig. 5a). This suggests that electrode fouling does not influence the secondary redox peaks significantly, making it an adequate method for the detection of BPA.

To enable accurate detection of BPA through this indirect method, we first oxidised BPA at a fixed potential of +0.6 V for a fixed time. We optimized the oxidation time to be around 60 s (SI Fig. 7), after which the secondary peak reached a plateau. We then used the standard curve method to detect BPA. First, we oxidised BPA at +0.6 V for 60 s followed by SWV. This step was repeated with sequential additions of BPA to the solution, resulting in a sequence of SWV curves (Fig. 6 a) and a calibration curve (Fig. 6 b). A new NC-GCE electrode was prepared and tested with known concentrations of BPA. The concentrations extrapolated using the linear relationship in Fig. 6 b are in close agreement with the added concentrations. A linear response between 0 and 80 μM ($R^2 > 0.99$) was obtained, which improved significantly compared with those extracted from the direct detection of BPA oxidation. The detection

Table 1
Sensors for BPA detection.

Sensors	Method	LOD (μM)	Detection Range (μM)	References
BDD	SWV	0.005	0–50	This work
Nanocarbon (direct)	SWV	0.56	0.5–30	This work
Nanocarbon (indirect)	SWV	0.062	0.1–80	This work
Carbon black/MWCNTs	Amperometry	0.08	0.1–130	[35]
SWCNT/GCE	Amperometry	7.3	10–100	[36]
graphene oxide/MWCNT	DPV	0.14	0.5–25	[37]
Casein/carbon black	LSV	0.25	0.49 to 24	[38]
PtSi/graphene/GCE	DPV	0.11	0.3–85	[39]
Carbon black/paper	SWV	0.03	0.1–0.9	[40]
Modified graphene oxide	DPV	0.017	0.2–10	[41]
Carbon black paste electrode	DPV	0.12	1–16	[42]
BDD	DPV	0.71	0.44–5.2	[43]
nanoporous gold leaf (NPGL)	SWV	0.06	0.3–100	[24]
FeNi ₃ /CuS/BiOCl	DPV	0.05	0.1–300	[44]
imprinted polyimide sheet	DPV	0.008	0.05–5	[45]
beta-CD/ionic liquid	DPV	0.083	0.1–11	[46]
PEDOT/ionic liquid	FIA	0.02	0.1–500	[47]

MWCNT: multiwalled carbon nanotubes.

SWCNT: single wall carbon nanotubes.

DPV: Differential pulse voltammetry.

LSV: linear sweep voltammetry.

SWV: square wave voltammetry.

limit can be calculated to be 0.062 μM with a sensitivity of 1.159 $\mu\text{A}\mu\text{M}^{-1}$ and noise of 24 nA.

In the interest of using this sensor in a context with several co-existing phenolic compounds, we show the simultaneous detection of phenolic compounds HQ, 1,2-dihydroxybenzene (DHB) and BPA using this indirect method (Fig. 7). Consecutive addition of BPA up to 5 μM showed distinguishable peaks for the three species, indicating the high selectivity of this nanocarbon sensor.

4. Conclusion

Mounting evidence suggests that BPA is more harmful to humans than expected. To tackle the challenges of tracking low levels of BPA, we developed electrochemical sensors based on carbon nanomaterials: nanodiamond and nanocarbon. In this work, we proposed three strategies, namely: the direct detection of BPA on boron-doped diamond electrodes and single-use nanocarbon electrodes, and the indirect detection of BPA through the redox reaction of the by-product quinone on nanocarbon electrodes. These methods detect BPA in a concentration range from 0.1 to 80 μM with a detection limit down to few nanomolar. The performance of these three methods exceeds many BPA sensors reported in the literature (summarised in Table 1). The carbon-based sensors presented in this work are capable of measuring BPA at concentrations lower than the daily dose limits set by recent medical advice.

In addition to a lower detection limit and wide detection range, the main feature of these three sensors are the avoidance of surface fouling, which is the main challenge for electrochemical BPA sensors.

This work offers different strategies that are suitable for various BPA detection situations, either developing a highly sensitive and reliable continuous BPA monitoring system, or an easy to use, low cost, BPA sensor. The former, based on the nanodiamond electrodes, can be used for portable on-site continuous BPA monitoring. The latter, based on nanocarbon electrodes, for single-use rapid tests and home use. We envisage that such sensors are promising tools to meet the challenges of BPA contamination and stricter regulations, as an alternative to the conventional ELISA tests or central lab equipment.

CRedit authorship contribution statement

Luyun Jiang: Formal analysis, Writing - original draft, design and implementation of the research. **Ibon Santiago:** Formal analysis, Writing - original draft, design and implementation of the research. **John Foord:** Formal analysis, Writing - original draft, design and implementation of the research.

Declaration of competing interest

The authors declare that they have no known competing financial interests or personal relationships that could have appeared to influence the work reported in this paper.

Acknowledgements

I.S. acknowledges the Alexander von Humboldt foundation for financial support.

Appendix A. Supplementary data

Supplementary data to this article can be found online at <https://doi.org/10.1016/j.carbon.2020.11.073>.

References

- [1] A.U. Alam, M.J. Deen, Bisphenol A electrochemical sensor using graphene oxide and β -cyclodextrin-functionalized multi-walled carbon nanotubes, *Anal. Chem.* 92 (7) (2020) 5532–5539. ISSN 0003–2700.
- [2] C. Karrer, W. de Boer, C. Delmaar, Y. Cai, A. Crépet, K. Hungerbühler, N. von Goetz, Linking probabilistic exposure and pharmacokinetic modeling to assess the cumulative risk from the bisphenols BPA, BPS, BPF, and BPAF for Europeans, *Environ. Sci. Technol.* 53 (15) (2019) 9181–9191. ISSN 0013–936X.
- [3] C. Erler, J. Novak, Bisphenol A exposure: human risk and health policy, *J. Pediatr. Nurs.* 25 (5) (2010) 400–407. ISSN 0882–5963.
- [4] Y.Q. Huang, C.K.C. Wong, J.S. Zheng, H. Bouwman, R. Barra, B. Wahlström, L. Neretin, M.H. Wong, Bisphenol A (BPA) in China: a review of sources, environmental levels, and potential human health impacts, *Environ. Int.* 42 (2012) 91–99. ISSN 0160–4120.
- [5] L. Canesi, E. Fabbri, Environmental effects of BPA: focus on aquatic species, *Dose-Response* 13 (3) (2015), 1559325815598304, ISSN 1559–3258.
- [6] P. Mirmira, C. Evans-Molina, Bisphenol A, obesity, and type 2 diabetes mellitus: genuine concern or unnecessary preoccupation? *Transl. Res.* 164 (1) (2014) 13–21. ISSN 1931–5244.
- [7] IRIS (Integrated Risk Information System), U.E.P.A. (EPA). <https://www.epa.gov/iris>.
- [8] Commission Regulation (EU) 2018/213 of 12 February 2018 on the use of bisphenol A in varnishes and coatings intended to come into contact with food and amending Regulation (EU) No 10/2011 as regards the use of that substance in plastic food contact materials (Text with EEA relevance.). <http://data.europa.eu/eli/reg/2018/213/oj>.
- [9] M. Montevil, N. Acevedo, C.M. Schaeberle, M. Bharadwaj, S.E. Fenton, A.M. Soto, A combined morphometric and statistical approach to assess nonmonotonicity in the developing mammary gland of rats in the CLARITY-BPA study, *Environ. Health Perspect.* 128 (5) (2020), 057001. ISSN 0091–6765.
- [10] Y. Yang, L. Lu, J. Zhang, Y. Yang, Y. Wu, B. Shao, Simultaneous determination of seven bisphenols in environmental water and solid samples by liquid chromatography–electrospray tandem mass spectrometry, *J. Chromatogr. A* 1328 (2014) 26–34. ISSN 0021–9673.
- [11] M. Horie, T. Yoshida, R. Ishii, S. Kobayashi, H. Nakazawa, Determination of bisphenol A in canned drinks by LC/MS, *Bunseki Kagaku* 48 (1999) 579–588. ISSN 0525–1931.
- [12] A. Zafra, M. del Olmo, B. Suarez, E. Hontoria, A. Navalon, J. L. Vilchez, Gas chromatographic–mass spectrometric method for the determination of bisphenol A and its chlorinated derivatives in urban wastewater, *Water Res.* 37.
- [13] H. Wang, Z.-h. Liu, Z. Tang, J. Zhang, H. Yin, Z. Dang, P.-x. Wu, Y. Liu, Bisphenol analogues in Chinese bottled water: quantification and potential risk analysis, *Sci. Total Environ.* 713 (2020) 136583. ISSN 0048–9697.
- [14] K. Wille, H.F. De Brabander, L. Vanhaecke, E. De Wulf, P. Van Caeter, C.R. Janssen, Coupled chromatographic and mass-spectrometric techniques for the analysis of emerging pollutants in the aquatic environment, *Trac. Trends Anal. Chem.* 35 (2012) 87–108. ISSN 0165–9936.
- [15] A. Kim, C.-R. Li, C.-F. Jin, K.W. Lee, S.-H. Lee, K.-J. Shon, N.G. Park, D.-K. Kim, S.-W. Kang, Y.-B. Shim, A sensitive and reliable quantification method for bisphenol A based on modified competitive ELISA method, *Chemosphere* 68 (7) (2007) 1204–1209. ISSN 0045–6535.
- [16] U.K. Şukriye, Sensitive voltammetric determination of bisphenol A based on a glassy carbon electrode modified with copper oxide-zinc oxide decorated on graphene oxide, *Electroanalysis* 31 (1) (2019) 91–102. ISSN 1040–0397.
- [17] L. Hu, C.-C. Fong, X. Zhang, L.L. Chan, P.K. Lam, P.K. Chu, K.-Y. Wong, M. Yang, Au nanoparticles decorated TiO₂ nanotube arrays as a recyclable sensor for photoenhanced electrochemical detection of bisphenol A, 0013–936X, *Environ. Sci. Technol.* 50 (8) (2016) 4430–4438.
- [18] D.-N. Pei, A.-Y. Zhang, X.-Q. Pan, Y. Si, H.-Q. Yu, Electrochemical sensing of bisphenol A on facet-tailored TiO₂ single crystals engineered by inorganic-framework molecular imprinting sites, *Anal. Chem.* 90 (5) (2018) 3165–3173. ISSN 0003–2700.
- [19] Y. Li, X. Zhai, X. Liu, L. Wang, H. Liu, H. Wang, Electrochemical determination of bisphenol A at ordered mesoporous carbon modified nano-carbon ionic liquid paste electrode, *Talanta* 148 (2016) 362–369. ISSN 0039–9140.
- [20] A. Thamilselvan, V. Rajagopal, V. Suryanarayanan, Highly sensitive and selective amperometric determination of BPA on carbon black/f-MWCNT composite modified GCE, *J. Alloys Compd.* 786 (2019a) 698–706. ISSN 0925–8388.
- [21] X. Li, C. Li, C. Wu, K. Wu, Strategy for highly sensitive electrochemical sensing: in situ coupling of a metal–organic framework with ball-mill-exfoliated graphene, *Anal. Chem.* 91 (9) (2019) 6043–6050. ISSN 0003–2700.
- [22] I. Kazane, K. Gorgy, C. Gondran, N. Spinelli, A. Zazoua, E. Defrancq, S. Cosnier, Highly sensitive bisphenol-A electrochemical aptasensor based on poly(pyrrole-nitrilotriacetic acid)-aptamer film, *Anal. Chem.* 88 (14) (2016) 7268–7273. ISSN 0003–2700.
- [23] L. Wu, X. Ji, J. Kong, Polymer-coated mesoporous carbon as enzyme platform for oxidation of bisphenol A in organic solvents, *ACS Omega* 4 (15) (2019) 16409–16417. ISSN 2470–1343.
- [24] R. Zhang, Y. Zhang, X. Deng, S. Sun, Y. Li, A novel dual-signal electrochemical sensor for bisphenol A determination by coupling nanoporous gold leaf and self-assembled cyclodextrin, *Electrochim. Acta* 271 (2018) 417–424. ISSN 0013–4686.

- [25] A. Ghanam, A.A. Lahcen, A. Amine, Electroanalytical determination of Bisphenol A: investigation of electrode surface fouling using various carbon materials, *J. Electroanal. Chem.* 789 (2017a) 58–66. ISSN 1572–6657.
- [26] E. Mahmoudi, A. Hajian, M. Rezaei, A. Afkhami, A. Amine, H. Bagheri, A novel platform based on graphene nanoribbons/protein capped Au-Cu bimetallic nanoclusters: application to the sensitive electrochemical determination of bisphenol A, *Microchem. J.* 145 (2019) 242–251. ISSN 0026–265X.
- [27] N. Yang, J.S. Foord, X. Jiang, Diamond electrochemistry at the nanoscale: a review, *Carbon* 99 (2016) 90–110. ISSN 0008–6223.
- [28] B.C. Lourencao, R.F. Brocenschi, R.A. Medeiros, O. Fatibello-Filho, R.C. Rocha-Filho, Analytical applications of electrochemically pretreated boron-doped diamond electrodes, *ChemElectroChem* 7 (6) (2020) 1291–1311.
- [29] L. Jiang, G.W. Nelson, J. Abda, J.S. Foord, Novel modifications to carbon-based electrodes to improve the electrochemical detection of dopamine, *ACS Appl. Mater. Interfaces* 8 (42) (2016) 28338–28348.
- [30] I. Shpilevaya, W. Smirnov, S. Hirs, N. Yang, C.E. Nebel, J.S. Foord, Nanostructured diamond decorated with Pt particles: preparation and electrochemistry, *RSC Adv.* 4 (2) (2014) 531–537.
- [31] L. Jiang, I. Santiago, J. Foord, Nanocarbon and nanodiamond for high performance phenolics sensing, *Commun. Chem.* 1 (1) (2018) 43. ISSN 2399–3669.
- [32] M. Gattrell, D. Kirk, A study of electrode passivation during aqueous phenol electrolysis, *J. Electrochem. Soc.* 140 (4) (1993) 903. ISSN 1945–7111.
- [33] P. Canizares, J. Lobato, R. Paz, M. Rodrigo, C. Sáez, Electrochemical oxidation of phenolic wastes with boron-doped diamond anodes, *Water Res.* 39 (12) (2005) 2687–2703.
- [34] M. Murugananthan, S. Yoshihara, T. Rakuma, T. Shirakashi, Mineralization of bisphenol A (BPA) by anodic oxidation with boron-doped diamond (BDD) electrode, *J. Hazard Mater.* 154 (1–3) (2008) 213–220.
- [35] A. Thamilselvan, V. Rajagopal, V. Suryanarayanan, Highly sensitive and selective amperometric determination of BPA on carbon black/f-MWCNT composite modified GCE, *J. Alloys Compd.* 786 (2019b) 698–706.
- [36] P. Kanagavalli, S. Senthil Kumar, Stable and sensitive amperometric determination of endocrine disruptor bisphenol A at residual metal impurities within SWCNT, *Electroanalysis* 30 (3) (2018) 445–452.
- [37] J.-S. Chen, Y. Li, M.-J. Yu, H.-L. Lee, Multiwalled carbon nanotubes/reduced graphene oxide nanocomposite electrode for electroanalytical determination of bisphenol A, 8-hydroxy-2'-deoxyguanosine and hydroquinone in urine, *Int. J. Environ. Anal. Chem.* 100 (7) (2020) 774–788.
- [38] L. Vieira Jodar, L.O. Orzari, T. Storti Ortolani, M.H. Assumpção, F.C. Vicentini, B.C. Janegitz, Electrochemical sensor based on casein and carbon black for Bisphenol A detection, *Electroanalysis* 31 (11) (2019) 2162–2170.
- [39] S. Zhang, Y. Shi, J. Wang, L. Xiao, X. Yang, R. Cui, Z. Han, Nanocomposites consisting of nanoporous platinum-silicon and graphene for electrochemical determination of bisphenol A, *Microchimica Acta* 187 (4) (2020) 1–8.
- [40] D. Jemmeli, E. Marcoccio, D. Moscone, C. Dridi, F. Arduini, Highly sensitive paper-based electrochemical sensor for a reagent free detection of bisphenol A, *Talanta* (2020) 120924.
- [41] Y. Wang, C. Li, T. Wu, X. Ye, Polymerized ionic liquid functionalized graphene oxide nanosheets as a sensitive platform for bisphenol A sensing, *Carbon* 129 (2018) 21–28.
- [42] A. Ghanam, A.A. Lahcen, A. Amine, Electroanalytical determination of Bisphenol A: investigation of electrode surface fouling using various carbon materials, *J. Electroanal. Chem.* 789 (2017b) 58–66.
- [43] G.F. Pereira, L.S. Andrade, R.C. Rocha-Filho, N. Bocchi, S.R. Biaggio, Electrochemical determination of bisphenol A using a boron-doped diamond electrode, *Electrochim. Acta* 82 (2012) 3–8.
- [44] M. Malakootian, S. Hamzeh, H. Mahmoudi-Moghaddam, A novel electrochemical sensor based on FeNi₃/CuS/BiOCl modified carbon paste electrode for determination of bisphenol A, *Electroanalysis*, 32, 1–9. <https://doi.org/10.1002/elan.202060205>.
- [45] T. Beduk, A.A. Lahcen, N. Tashkandi, K.N. Salama, One-step electrosynthesized molecularly imprinted polymer on laser scribed graphene bisphenol a sensor, *Sensor. Actuator. B Chem.* (2020) 128026.
- [46] X. Yu, Y. Chen, L. Chang, L. Zhou, F. Tang, X. Wu, beta-cyclodextrin non-covalently modified ionic liquid-based carbon paste electrode as a novel voltammetric sensor for specific detection of bisphenol A, *Sensor. Actuator. B Chem.* 186 (2013) 648–656.
- [47] J.-Y. Wang, Y.-L. Su, B.-H. Wu, S.-H. Cheng, Reusable electrochemical sensor for bisphenol A based on ionic liquid functionalized conducting polymer platform, *Talanta* 147 (2016) 103–110.